



Research Article

Genetic analysis of human adenovirus type 108 circulating in China during 2014–2024



Jinjin Wang^a, Ling Jing^b, Yali Duan^a, Junhong Ai^a, Yun Zhu^a, Ran Wang^a, Xiangpeng Chen^a, Gen Lu^c, Yun Sun^d, Changchong Li^e, Rong Jin^f, Yunxiao Shang^g, Yixiao Bao^h, Shuhua Anⁱ, Yunlian Zhou^j, Limin Ning^k, Baoping Xu^l, Yuhai Bi^{m,n,o}, Zhengde Xie^{a,*}

^a Beijing Key Laboratory of Core Technologies for the Prevention and Treatment of Emerging Infectious Diseases in Children, Key Laboratory of Major Diseases in Children, Ministry of Education, National Clinical Research Center for Respiratory Diseases, Research Unit of Critical Infection in Children, Chinese Academy of Medical Sciences, 2019RU016, Laboratory of Infection and Virology, Beijing Pediatric Research Institute, Beijing Children's Hospital, Capital Medical University, National Center for Children's Health, Beijing, 100045, China

^b Institute of Pathogen Biology, Chinese Academy of Medical Sciences & Peking Union Medical College, Beijing, 102629, China

^c Department of Respiratory, GuangZhou Women and Children's Medical Center, GuangZhou, 510623, China

^d Department of General Pediatrics, Yinchuan Women and Children Healthcare Hospital, Yinchuan, 750002, China

^e Department of Respiratory, The 2nd Affiliated Hospital and Yuying Children's Hospital of Wenzhou Medical University, Wenzhou, 325027, China

^f Department of Respiratory, Guiyang Maternal and Child Health Hospital, Guiyang, 550003, China

^g Department of Pediatric Respiratory, Shengjing Hospital of China Medical University, Shenyang, 110004, China

^h Xin Hua Hospital Affiliated to Shanghai Jiao Tong University School of Medicine, Shanghai, 200092, China

ⁱ Children's Hospital of Hebei Province, Shijiazhuang, 050031, China

^j The Children's Hospital, Zhejiang University School of Medicine, Hangzhou, 310052, China

^k Children's Hospital of Changchun, Changchun, 130061, China

^l National Clinical Research Center for Respiratory Diseases, Department of Respiratory Medicine, Beijing Children's Hospital, Capital Medical University, National Center for Children's Health, Beijing, 100045, China

^m College of Veterinary Medicine, Shanxi Agricultural University, Jinzhong, 030801, China

ⁿ CAS Key Laboratory of Pathogen Microbiology and Immunology, Institute of Microbiology, Center for Influenza Research and Early-warning (CASCIRE), CAS-TWAS Center of Excellence for Emerging Infectious Diseases (CEEID), Chinese Academy of Sciences (CAS), Beijing, 100101, China

^o University of Chinese Academy of Sciences, Beijing, 100049, China

ARTICLE INFO

Keywords:

Human adenovirus type 108 (HAdV-108)

Acute respiratory infection (ARI)

Clinical characteristics

Genetic characteristics

Children

ABSTRACT

Human adenovirus type 108 (HAdV-108) has been detected in multiple countries, including China, and is associated with severe acute respiratory infection (ARI) in children, with reported fatalities. However, studies on HAdV-108 remain limited. This study aimed to investigate the clinical and genetic characteristics of HAdV-108 in ARI children in China. From 2014 to 2024, 6720 respiratory samples were collected from hospitalized children with ARI at ten hospitals across northern and southern China, of which 505 (7.51%) tested positive for HAdV. The whole-genome and three major capsid protein genes were amplified and sequenced for bioinformatics analysis, which revealed that among 317 HAdV-isolated samples, 21 (6.62%) were identified as HAdV-108, ranking third after HAdV-114 and HAdV-7. Clinical analysis of HAdV-108-positive cases showed that the main manifestations were cough and fever. Seven children had gastrointestinal symptoms, and two children without underlying diseases were diagnosed with severe pneumonia. Phylogenetic analysis of whole-genome sequences revealed distinct predominant epidemic branches between domestic and international strains, with one strain obtained in this study forming an independent branch. Hexon protein exhibited the fastest evolution rate, lowest identity, and greatest amino acid variability, while fiber protein displayed the slowest evolution rate, highest identity, and greatest conservation and stability. Compared with the earliest reported HAdV-108 strain, three amino acid deletions were identified in the RGD loop region of penton base protein, resulting in potential structural change. Recombination

* Corresponding author.

E-mail address: xiezhengde@bch.com.cn (Z. Xie).

<https://doi.org/10.1016/j.virs.2025.09.002>

Received 17 April 2025; Accepted 11 September 2025

Available online 19 September 2025

1995-820X/© 2025 The Authors. Publishing services by Elsevier B.V. on behalf of KeAi Communications Co. Ltd. This is an open access article under the CC BY-NC-ND license (<http://creativecommons.org/licenses/by-nc-nd/4.0/>).

analysis identified five distinct recombination patterns. *In vitro* experiments demonstrated that HAdV-108 had proliferation capacity comparable to other species C adenoviruses. In summary, HAdV-108 has persistently circulated in China, causing severe ARIs and concurrent gastrointestinal manifestations. Cluster3 was the predominant epidemic branch in China. HAdV-108 exhibited significant intra-type genetic variation, with random and diverse recombination events.

INTRODUCTION

Human adenovirus (HAdV), initially discovered and isolated from children's adenoids by Rowe in 1953 (Rowe et al., 1953), belongs to the *Mastadenovirus* genus of the *Adenoviridae* family. It is a nonenveloped, linear double-stranded deoxyribonucleic acid (DNA) virus with a diameter ranging from 70 to 100 nm and a total genome length of approximately 34–36 kb (Li et al., 2018). The capsid of the HAdV is icosahedral symmetric and composed of three major capsid proteins (penton base, hexon, and fiber), in addition to several minor capsid proteins (Davison et al., 2003). Penton base protein harbors two pivotal sites: the Arg-Gly-Asp (RGD) loop and the hypervariable region (HVR) 1 region. The RGD loop is situated within the hypervariable loop 2 region and mediates the interaction with the integrin expressed on the host cell surface, facilitating the virus internalization and infection (Davison et al., 2003). The HVR1 is located on the surface of the virus capsid, and recombination can occur at this site and its vicinity (Madisch et al., 2007). Hexon protein is the key antigenic protein of HAdV and can induce the host's immune response (Zhu and Mao, 2022). It comprises two hypervariable circular domains: Loop1 (including HVR1–6) and Loop2 (including HVR7), which are primary targets for inducing neutralizing antibodies and form ϵ antigen epitopes. The ϵ antigen epitopes are highly sensitive to the immune selection pressure, exhibiting species- and type-specific characteristics. They form the foundation for virus serum neutralization experiments and type identification (Zhu and Mao, 2022; Madisch et al., 2005). Components of fiber protein include N-terminal tail (Tail), stalk (Shaft), and C-terminal spherical domain nodules (Knob). The Knob region plays a crucial role in facilitating virus attachment by mediating the interaction between HAdV and the receptor on the host cell surface (Liu et al., 2023).

HAdV has been classified into 7 species from A to G to date, with a total of 116 types (<http://hadv.wg.gmu.edu/>). Recombination and immune selection are considered the primary driving forces behind HAdV diversity (Ismail et al., 2018). Different types of HAdVs exhibit distinct tissue tropism and can cause different diseases (Wu et al., 2025). HAdV is a key pathogen responsible for acute respiratory infection (ARI) in children, with a detection rate ranging from 0.25% to 26.77% (Wang et al., 2023; Huang et al., 2023; Mahmood et al., 2024; Saha et al., 2023). In children with severe ARIs, the detection rate of HAdV can be as high as approximately 29% (Bezerra et al., 2011), with potential fatalities following infection (Wei et al., 2023). HAdV-C (including HAdV-1, -2, -5, -6, -57, -89, -104, -108) is widely prevalent and considered as one of the primary pathogens causing respiratory tract infection in pediatric patients (Yang et al., 2019). It contributes to about 5% of upper respiratory tract infection (URTI) and approximately 15% of lower respiratory tract infection in children under 5 years old (Takahashi et al., 2019). Moreover, it is associated with outbreaks of HAdV-induced acute respiratory viral infections in children (Zhao et al., 2020; Dhingra et al., 2019).

HAdV-108 is a member of species C. It is an interspecific recombinant virus and also designated P1H2F2 according to the current nomenclature protocol primarily following the system proposed by the international HAdV Working Group (Seto et al., 2011), which defines genotypes based on the nucleotide sequences of the *penton base*, *hexon*, and *fiber* genes. Genome sequence analysis revealed that HAdV-108 was generated by replacing the entire *penton base* gene (approximately

1700–1800 bp, accounting for about 5% of the whole genome) of HAdV-2 with the *penton base* gene from HAdV-1 (Roberts et al., 1984; Wang et al., 2024). Initially, HAdV-108 was misclassified as HAdV-2 based on serum neutralization and hemagglutination inhibition tests by detecting antigenic epitopes in hexon and fiber proteins or limited sequencing. With the advent of whole-genome sequencing, which transformed HAdV typing, it was not confirmed as a novel type until 2014 (<http://hadv.wg.gmu.edu/>). Subsequently, it has been identified in multiple countries, including China, USA and Russia (Wang et al., 2024; Kurskaya et al., 2024). So far, the earliest reported strain of HAdV-108, the SX-2000-140 strain (GenBank accession number: MK165452), was isolated from Shanxi, China in 2000, suggesting a longstanding presence of HAdV-108 in Chinese mainland (Yang et al., 2019).

HAdV-108 infection can cause severe illnesses in children, with documented fatalities, particularly among those with compromised immune function (Wang et al., 2016; Becken et al., 2024). Wang et al. isolated an HAdV-108 strain from a child hospitalized with severe ARI in Beijing, China in 2009 (Wang et al., 2016). Cai et al. found that the detection rate of HAdV-108 was 9.8% among all HAdV-positive samples from children hospitalized with severe ARI in eight provinces across northern and southern China during 2017–2021, ranking fourth after HAdV-1, -3, and -7 (Cai et al., 2024). In 2024, Becken et al. reported a case involving a 3-year-old boy with X-linked lymphoproliferative syndrome who underwent an unrelated umbilical cord blood transplant. Subsequently, there was a gradual elevation in HAdV-108 viral load in his blood, which ultimately led to liver dysfunction and mortality six months post-transplant (Becken et al., 2024). Wu et al. found that the detection rate of HAdV-108 was 7.33% among all HAdV-positive samples from children hospitalized with ARI in Wuhan from 2022 to 2023, ranking second only to HAdV-3. Additionally, 36.36% of these children infected with HAdV-108 developed sepsis (Wu et al., 2025). Recently, studies have identified diverse recombination patterns in HAdV-108, with inconsistent genomic evolutionary diversity and notable genetic variation among different sequences (Becken et al., 2024). Yang et al. discovered significant differences in the 5' end of HAdV-108 sequences between strains obtained from Shanxi, China in 2000 and 2004, and those from Beijing, China in 2009 and 2013, indicating a potential recombination event in that region (Yang et al., 2019). Cheng found that the HAdV-108 strains identified at Wuwei People's Hospital in Gansu, China in 2021 were formed by recombination of HAdV-1, -89 and -104 in the *E1B*, *E2B* and *E4* regions (Cheng, 2024). Lei et al. identified two distinct HAdV-108-related recombination variants circulating in Tianjin, China between 2021 and 2022: One used HAdV-2 as the backbone, with the genes between *E1A* and DNA polymerase genes embedded with HAdV-5, while the genes between DNA polymerase and the pre-protein VI genes (including *penton base* gene) originating from HAdV-1. The other comprised the *penton base* gene of HAdV-1 and the *hexon* and *fiber* genes of HAdV-2. Additionally, partial sequences of DNA polymerase and *E4* open reading frame 1 originated from HAdV-6 and HAdV-5, respectively (Lei et al., 2023).

To date, there is a scarcity of sequences of HAdV-108 strains worldwide, including China. There are only 35 whole genome sequences of HAdV-108 in public databases [including 30 sequences in GenBank and 5 sequences in China National Microbiology Data Center (NMDC)], 19 sequences of which are from China. Furthermore, due to its recent classification as a novel type, researches on HAdV-108 are scant, leading

to limited understanding of its molecular genetic characteristics and evolutionary history in China. Currently, no safe and effective drugs or vaccines against HAdV-108 are available. This study aimed to elucidate the clinical and genetic characteristics of HAdV-108 in China, providing a data reference for the surveillance, prevention and control of HAdV-108, as well as for advancements in vaccine and drug development. Children with ARI admitted to 10 hospitals across 9 provinces in northern and southern China from 2014 to 2024 were included in this study. Clinical data of HAdV-108-positive patients were collected and analyzed to determine their clinical characteristics. Bioinformatics analyses were performed on the whole genome sequences, as well as the *penton base*, *hexon*, and *fiber* gene sequences.

RESULTS

Detection rate of HAdV-108

A total of 6720 ARI children were enrolled into this study, of which 505 (7.51%) HAdV-positive samples were detected (Fig. 1). Three hundred and seventeen HAdV-positive samples were successfully isolated and genotyped. Three species (including 15 genotypes) were identified: B (HAdV-3, -7, -11, -14, -21, -55, -66, and -114), C (HAdV-1, -2, -5, -6, -89, and -108), and E (HAdV-4). Furthermore, three additional gene recombination patterns (P7H3F7, P89H5F5, P5H1F1) were identified. HAdV-114, -7, -108, and -1 were the most identified types, with

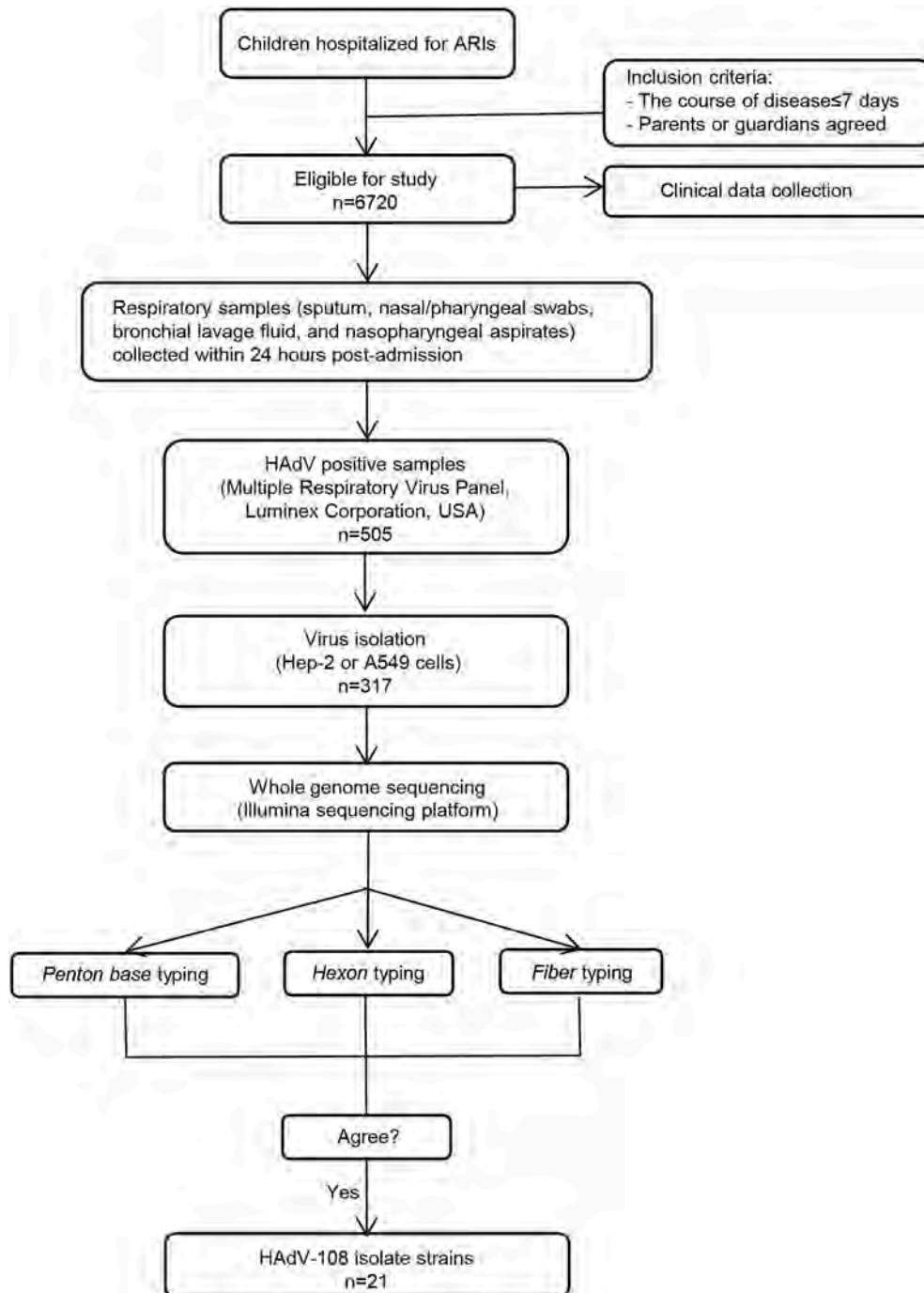


Fig. 1. Flow diagram of the study. Agree: The typing results based on the penton base, hexon, and fiber genes were all consistent with HAdV-108 (P1H2F2). Specifically, P1H2F2 indicates that the penton base is derived from HAdV-1, whereas the hexon and fiber are derived from HAdV-2.

149 (47.00%), 91 (28.71%), 21 (6.62%), and 15 (4.73%) strains, respectively. However, only one (0.32%) strain of HAdV-2 was identified. The detailed information of the 21 HAdV-108-positive samples is provided in [Supplementary Table S1](#). There was 1 case (4.76%, 1/21) in 2017, 6 cases (28.57%, 6/21) in 2018, 3 cases (14.29%, 3/21) in 2019, 1 case (4.76%, 1/21) in each year from 2020 to 2023, and 7 cases (33.33%, 7/21) with missing specific collection time information.

Clinical characteristics of patients with HAdV-108 infection

The clinical characteristics of 21 patients with HAdV-108 infection are shown in [Supplementary Table S2](#). Fifteen children (71.43%, 15/21) were diagnosed with pneumonia, two children (9.52%, 2/21) with bronchitis, and four children (19.05%, 4/21) with URTI. Seven children lacked detailed clinical data. Among the remaining 14 children with detailed clinical data, ten children (71.43%, 10/14) had cough and ten children (71.43%, 10/14) developed fever peaking at 39–40.1 °C. Five children (35.71%, 5/14) had sputum secretion, and 7 children (50%, 7/14) exhibited gastrointestinal symptoms such as abdominal pain, diarrhea, vomiting, and so on. Two (14.29%, 2/14) children without underlying diseases developed wheezing and dyspnea, culminating in a severe pneumonia diagnosis. One of them progressed to respiratory failure and necessitated nasal continuous positive airway pressure respiratory support. This patient experienced severe complications like electrolyte disturbance, liver function damage, myocardial damage, neutropenia, etc. and was admitted to the pediatric intensive care unit (PICU), with the longest hospital stay. Both children were not coinfecting with other viruses. Hospitalization durations ranged from 2 to 25 days. All patients improved and were discharged without any deaths.

Of the 16 children with HAdV-1 or -2 infections, only 14 children obtained detailed clinical data. When comparing the clinical characteristics of children infected with HAdV-1/2 to those with HAdV-108, wheezing was more common in the children infected with HAdV-1/2 ($P = 0.038$), while abdominal pain was more frequent in the children with HAdV-108 infection ($P = 0.02$). No statistically significant differences were observed in other clinical manifestations, diagnoses, complications, oxygen support, PICU admission, length of hospitalization, or mortality ([Table 1](#)).

Table 1
Comparison of clinical characteristics of children infected with HAdV-1/2 or HAdV-108.

	HAdV-1/2	HAdV-108	χ^2	<i>P</i>
Demographic				
Gender (male/female)	6/10	13/7	1.707	0.191
Age (median, years)	1.915	2.29		0.739
Clinical manifestation				
Fever	11 (78.57%)	10 (71.43%)	1.000	0.500
Cough	12 (85.71%)	10 (71.43%)	0.648	0.324
Sputum secretion	10 (71.43%)	5 (35.71%)	0.128	0.064
Wheezing	6 (42.86%)	1 (7.14%)	0.077	0.038
Dyspnea	5 (35.71%)	2 (14.29%)	0.385	0.192
Abdominal pain	0	5 (35.71%)	0.041	0.02
Diarrhea	3 (21.43%)	1 (7.14%)	0.596	0.298
Vomiting	4 (28.57%)	1 (7.14%)	0.326	0.163
Clinical diagnosis				
Pneumonia	11 (68.75%)	15 (71.43%)	1.000	0.571
Severe pneumonia	1 (6.25%)	2 (9.52%)	1.000	0.604
Suppurative tonsillitis	2 (12.50%)	2 (9.52%)	1.000	0.587
Bronchitis	4 (25.00%)	2 (9.52%)	0.371	0.207
Complication				
Respiratory failure	0	1 (7.14%)	1.000	0.500
Electrolyte disturbance	4 (28.57%)	1 (7.14%)	0.326	0.163
Liver function damage	4 (28.57%)	2 (14.29%)	0.648	0.324
Myocardial damage	6 (42.86%)	2 (14.29%)	0.209	0.104
Oxygen support	5 (35.71%)	1 (7.14%)	0.165	0.082
Pediatric intensive care unit admission	1 (7.14%)	1 (7.14%)	1.000	0.759
Hospitalization (median, days)	8	7.5		0.722
Mortality	0	0		

Identification of HAdV-108

Reference sequences for the whole genome, *penton base*, *hexon*, and *fiber* genes of prototype or representative strains of other types within species C were retrieved from GenBank ([Supplementary Table S3](#)).

Phylogenetic analysis of the whole genome confirmed that the 21 strains obtained in this study all belonged to species C and clustered with HAdV-108 ([Fig. 2A](#)). Sequence analysis of the *penton base* gene showed that these 21 strains clustered with HAdV-1, -57, and -104 within the HAdV-1 evolutionary branch ([Fig. 2B](#)). For the *hexon* gene, the 21 strains clustered with HAdV-2 and -108 within the HAdV-2 evolutionary branch, including HAdV-89 ([Fig. 2C](#)). The *fiber* gene phylogenetic analysis revealed that these strains clustered with HAdV-2, -89, -104, and -108 within the HAdV-2 evolutionary branch ([Fig. 2D](#)). Based on these findings, the 21 strains could be identified as HAdV-108, designated P1H2F2.

Phylogenetic analysis of the whole genome of HAdV-108

Twenty-one HAdV-108 strains were isolated, and their whole genome sequences were obtained ([Supplementary Table S1](#)), with the nucleotide sequence identity of 98.6%–99.9% and the genetic distance of 0.006. Thirty-five whole genome reference sequences of HAdV-108 were obtained ([Supplementary Table S3](#)) from GenBank ($n = 30$) and NMDC ($n = 5$).

The whole genome sequence phylogenetic analysis showed that HAdV-108 could be divided into four evolutionary branches. Cluster1 comprised strains isolated in USA from 2009 to 2016, while a few whole genome sequences from this study clustered with those identified in the early years in USA, forming Cluster2. Among the reference strains from China, only the BJ04 strain (GenBank accession number: MF315028) isolated from Beijing in 2012 was located in Cluster2. The majority of the isolates obtained in this study, as well as all previously reported HAdV-108 strains from China (except for the BJ04 strain), were situated in Cluster3, along with the strains isolated from USA and Russia in recent years. All strains identified worldwide from 2020 onwards belonged to Cluster3. One strain obtained in this study, the BX-2024-1201/BX strain, formed a distinct phylogenetic branch (Cluster4)

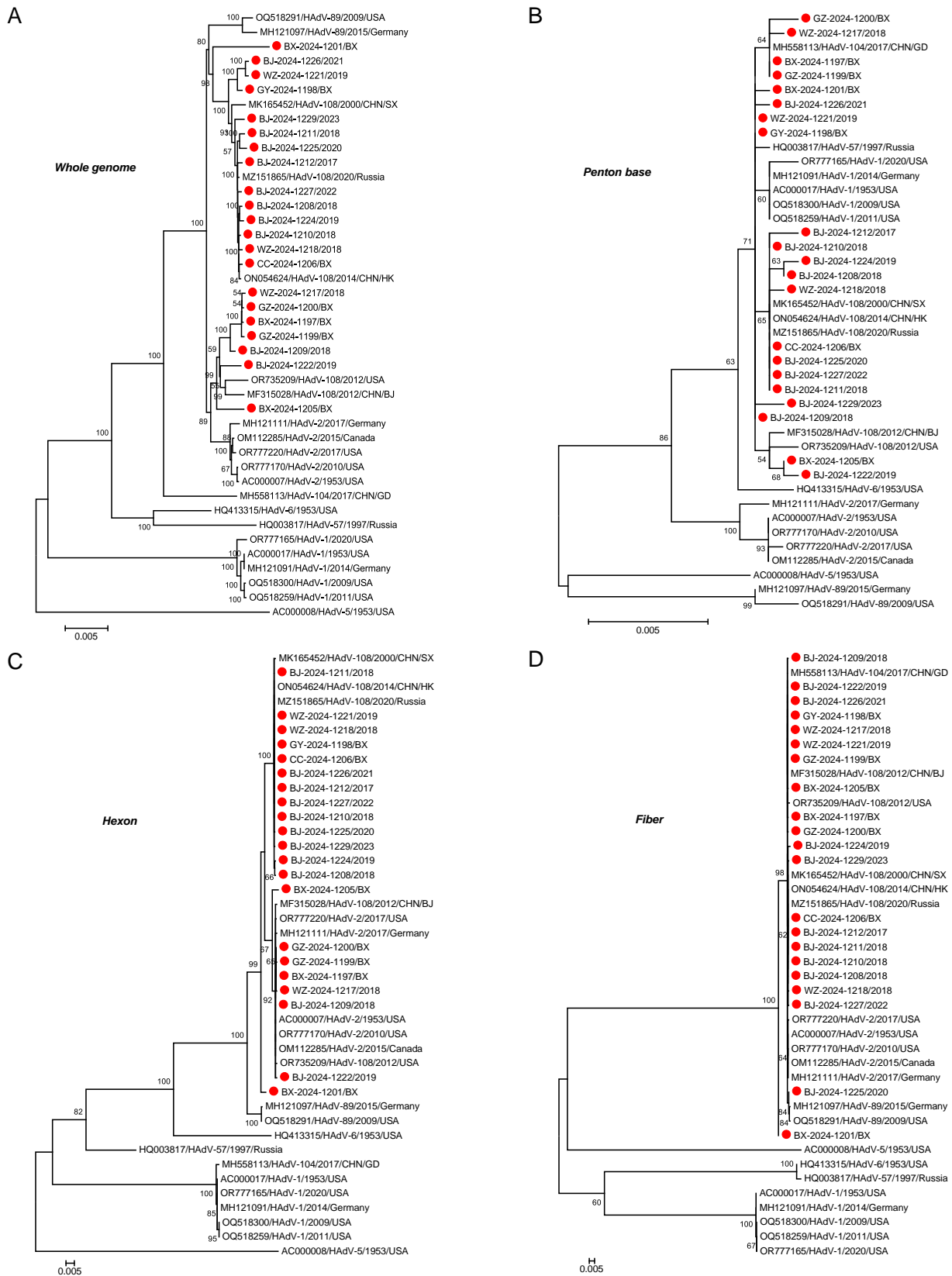


Fig. 2. Phylogenetic analysis of the whole genome and three major capsid protein genes of the 21 HAdV-108 strains and other types within species C. The phylogenetic trees of the whole genome (A) and *penton base* gene (B) were constructed by the Maximum Likelihood method and the Tamura 3-parameter model using 1000 replicates. The phylogenetic tree of *hexon* gene (C) was constructed by the Maximum Likelihood method and the General Time Reversible model using 1000 replicates. The phylogenetic tree of *fiber* genes (D) was constructed by the Maximum Likelihood method and the Hasegawa-Kishino-Yano model using 1000 replicates. Red dots indicate the 21 HAdV-108 strains obtained in this study.

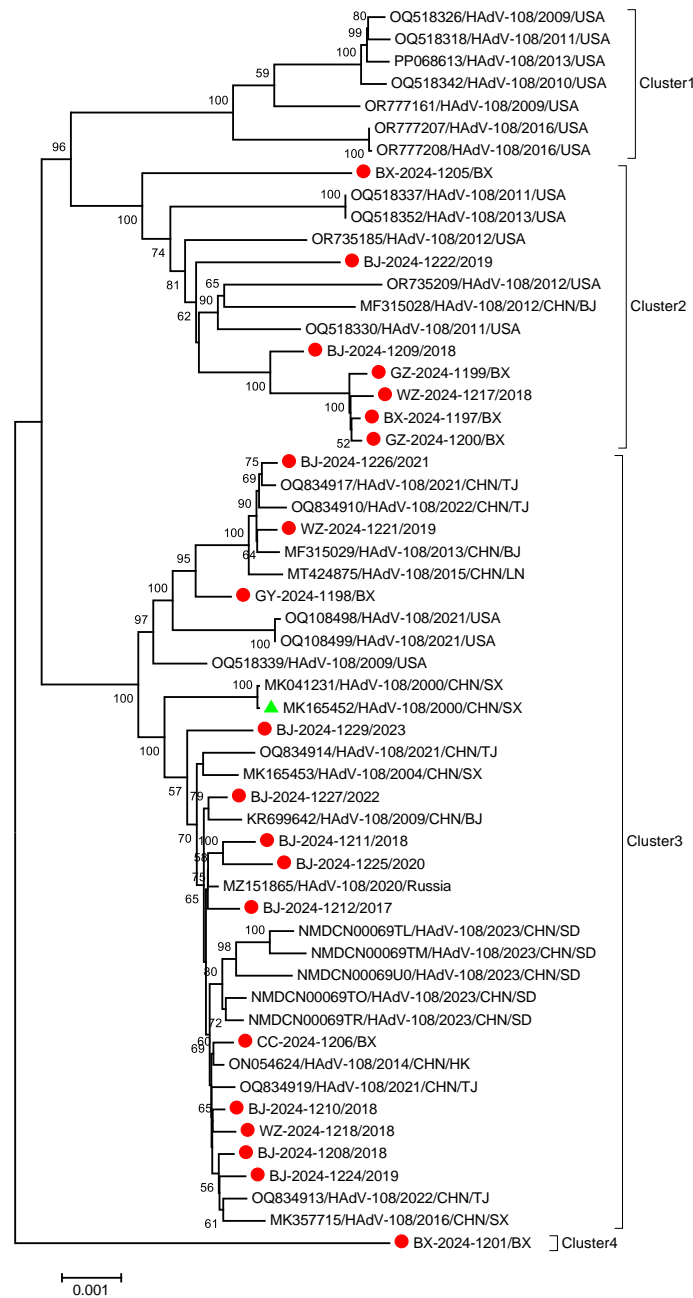


Fig. 3. Phylogenetic analysis of the whole genome of HAdV-108. The phylogenetic tree was constructed by the Maximum Likelihood method and the Tamura 3-parameter model using 1000 replicates. Cyan triangle indicates the SX-2000-140 strain (the earliest reported strain of HAdV-108, GenBank accession number: MK165452). Strains obtained in this study are indicated by red dots.

independently (Fig. 3). The nucleotide sequence identity on the whole genome sequences of all HAdV-108 strains from China were 96.2%–99.9%, with the genetic distance of 0.005. The mean genetic distances within the group of Cluster1, Cluster2 and Cluster3 were 0.003, 0.005 and 0.003, respectively. The mean genetic distances between the groups of Cluster1 and Cluster2, Cluster1 and Cluster3, Cluster1 and Cluster4 were 0.010, 0.009 and 0.012, respectively. The mean genetic distances between the groups of Cluster2 and Cluster3, Cluster2 and Cluster4, Cluster3 and Cluster4 were 0.009, 0.011 and 0.010, respectively.

Phylogenetic analysis of the penton base, hexon, and fiber genes

Base on the sequences of *penton base*, *hexon*, and *fiber* genes of 21 HAdV-108 strains isolated in this study (Supplementary Table S1), as

well as 35 reference sequences of each gene from GenBank and China NMDC (Supplementary Table S3), the nucleotide and amino acid sequence identities, along with genetic distances are compared in Table 2.

The phylogenetic analysis of *penton base* gene sequences of HAdV-108 revealed three distinct evolutionary branches (Fig. 4A). Most of the sequences obtained in this study, together with historical Chinese HAdV-108 strains (excluding the BJ04 strain), were affiliated with Cluster3, which also encompassed strains isolated from USA and Russia in recent years. Importantly, all sequences worldwide from 2020 onwards were located in Cluster3. Two sequences obtained in this study clustered with two strains isolated from USA between 2011 and 2012, as well as the BJ04 strain, forming Cluster2. Cluster1 consisted of strains found in USA from 2009 to 2016. The mean genetic distances within the

Table 2
Evolutionary divergences among the three major capsid protein genes of HAdV-108.

		HAdV-108 strains obtained in this study (n = 21)			HAdV-108 strains obtained in China (n = 40)			HAdV-108 strains worldwide (n = 56)		
		Penton base	Hexon	Fiber	Penton base	Hexon	Fiber	Penton base	Hexon	Fiber
Identity (%)	DNA ^a	99.6–100	98.7–100	98.9–100	95.8–100	93.5–100	98.9–100	95.5–100	92.3–100	98.9–100
	AA ^a	99.4–100	99.6–100	98.7–100	95.6–100	94.6–100	98.7–100	95.2–100	94.6–100	98.6–100
Mean genetic distance	DNA	0.001	0.006	0.002	0.002	0.005	0.002	0.003	0.010	0.002
	AA	0.001	0.000	0.003	0.002	0.000	0.002	0.003	0.002	0.003

Note: ^a DNA: Deoxyribonucleic Acid; AA: Amino acid.

group of Cluster1, Cluster2 and Cluster3 were 0.002, respectively. The mean genetic distances between the groups of Cluster1 and Cluster2, Cluster1 and Cluster3, Cluster2 and Cluster3 were 0.005, 0.005 and 0.002, respectively.

Based on the phylogenetic analysis of *hexon* gene sequences of HAdV-108, there were four phylogenetic branches (Fig. 4B), consistent with the results of the whole genome sequence phylogenetic analysis. Sequences obtained in USA from 2009 to 2016 formed Cluster1. Several sequences obtained in this study clustered with the early USA strains and the BJ04 strain found in Beijing, China in 2012, forming Cluster2. The majority of the sequences obtained in this study, as well as all known HAdV-108 strains from China (except for the BJ04 strain) were located in Cluster3, along with the strains isolated from USA and Russia in recent years. The BX-2024-1201/BX strain obtained in this study independently branched off to form Cluster4. All sequences worldwide from 2020 onwards were located in Cluster3. The mean genetic distances within the group of Cluster1, Cluster2 and Cluster3 were 0.000, 0.002 and 0.002, respectively. The mean genetic distances between the groups of Cluster1 and Cluster2, Cluster1 and Cluster3, Cluster1 and Cluster4 were 0.022, 0.024 and 0.019, respectively. The mean genetic distances between the groups of Cluster2 and Cluster3, Cluster2 and Cluster4, Cluster3 and Cluster4 were 0.012, 0.009 and 0.010, respectively.

The phylogenetic analysis of *fiber* gene sequences showed that HAdV-108 could be divided into four evolutionary branches (Fig. 4C). The BJ-2024-1225/2020 strain obtained in this study and strains isolated from USA between 2009 and 2016 formed Cluster1. Seven sequences obtained in this study clustered with those reported in USA during 2011–2013 and the BJ04 strain found in Beijing, China in 2012, forming Cluster2. The majority of the sequences obtained in this study, alongside previously identified HAdV-108 strains from China (excluding the BJ04 strain), and strains isolated from USA in 2009 and 2021, as well as the strain discovered in Russia in 2020 (GenBank accession number: MZ151865), were clustered in Cluster3. The BX-2024-1201/BX strain identified in this study independently diverged to form a distinct phylogenetic branch (Cluster4). The mean genetic distances within the group of Cluster1, Cluster2 and Cluster3 were 0.001, respectively. The mean genetic distances between the groups of Cluster1 and Cluster2, Cluster1 and Cluster3, Cluster1 and Cluster4 were 0.003, 0.003 and 0.010, respectively. The mean genetic distances between the groups of Cluster2 and Cluster3, Cluster2 and Cluster4, Cluster3 and Cluster4 were 0.002, 0.009 and 0.009, respectively. The mean genetic distances of amino acids of the three major capsid proteins were close. However, the nucleotide and amino acid identities of hexon were the lowest, with the farthest mean genetic distance of nucleotides. In contrast, the nucleotide and amino acid identities of fiber were the highest, and the mean genetic distance was small (Table 2).

Amino acid variation analysis

Compared with the SX-2000-140 strain (GenBank accession number: MK165452), HAdV-108 strains worldwide, including the 21 strains obtained in this study, had no amino acid mutation in the HVRI region of penton base protein. Three amino acid deletions (E367, A368 and

A369) and one amino acid substitution (S386T) were observed in the RGD loop region of penton base protein (Fig. 5A). The deletions were unique to the sequences obtained in this study and five strains isolated from Shandong, China in 2023 (NMDC accession numbers: NMDCN00069TO, NMDCN00069TR, NMDCN00069UO, NMD CN00069TL, and NMDCN00069TM). According to the phylogenetic analysis of *penton base* gene sequences, HAdV-108 was divided into three evolutionary branches. The substitution (S386T) was present in Cluster1 and Cluster2, as well as all strains discovered in USA, including those in Cluster3. Moreover, it was also found in some sequences of Cluster3, including partial sequences obtained in this study. Furthermore, two additional cluster-specific amino acid substitutions were found in Cluster1: A420T and S458R. However, based on the whole genome sequence phylogenetic analysis, HAdV-108 was divided into four evolutionary branches. The substitution was present in Cluster1, 2 and 4. Besides, it was also found in some sequences of Cluster3, including four sequences obtained in this study (GY-2024-1198/BX, WZ-2024-1221/2019, BJ-2024-1226/2021 and BJ-2024-1229/2023), all strains discovered in USA and several strains isolated from northern China (Fig. 5A). No additional cluster-specific amino acid mutations were observed.

In comparison with the SX-2000-140 strain, all sequences discovered in China, including the 21 sequences obtained in this study, had no amino acid mutation in the Loop1 and Loop2 regions of hexon protein. Nevertheless, one amino acid insertion (I49E) and one amino acid substitution (M306L) were present in the Loop1 region, along with two amino acid substitutions (S449A, D454 N) in the Loop2 region (Fig. 5A). Based on *hexon* gene sequences analysis, HAdV-108 was divided into four evolutionary branches, consistent with the results of the whole genome sequence phylogenetic analysis. These mutations were specific to Cluster1 and absent in other clusters. Moreover, two additional cluster-specific amino acid substitutions were found in Cluster1: E830D, L837I (Fig. 5A). Selection pressure analysis showed that hexon protein contained a negative selection site 763 (K). No positive selection site was found.

Compared with the SX-2000-140 strain, the sequences obtained in this study did not have any amino acid mutations in the Knob region of fiber protein, except for the BX-2024-1201/BX and the BJ-2024-1227/2022 strains. The former displayed three amino acid substitutions (D444 N, I531T, E547Q), whereas the latter had one amino acid substitution (S546G) (Fig. 5A). The amino acid substitution (E547Q) was also found in the SX-2004-327 strain isolated from Shanxi, China in 2004 (GenBank accession number: MK165453), while a different amino acid substitution (E547K) was observed at the same site in the strain discovered in Tianjin, China in 2021 (GenBank accession number: OQ834919). Based on the phylogenetic analysis of *fiber* gene sequences, HAdV-108 was divided into four evolutionary branches, generally concordant with the results of the whole genome sequence phylogenetic analysis. An amino acid substitution (N171D) was found in Cluster1, 2 and 4, as well as in all strains discovered in USA, including those in Cluster3. In addition, it was also observed in some sequences of Cluster3, including partial sequences obtained in this study. Furthermore, two additional amino acid substitutions were present in the BX-2024-1201/BX strain: S208G and Q232E (Fig. 5A).

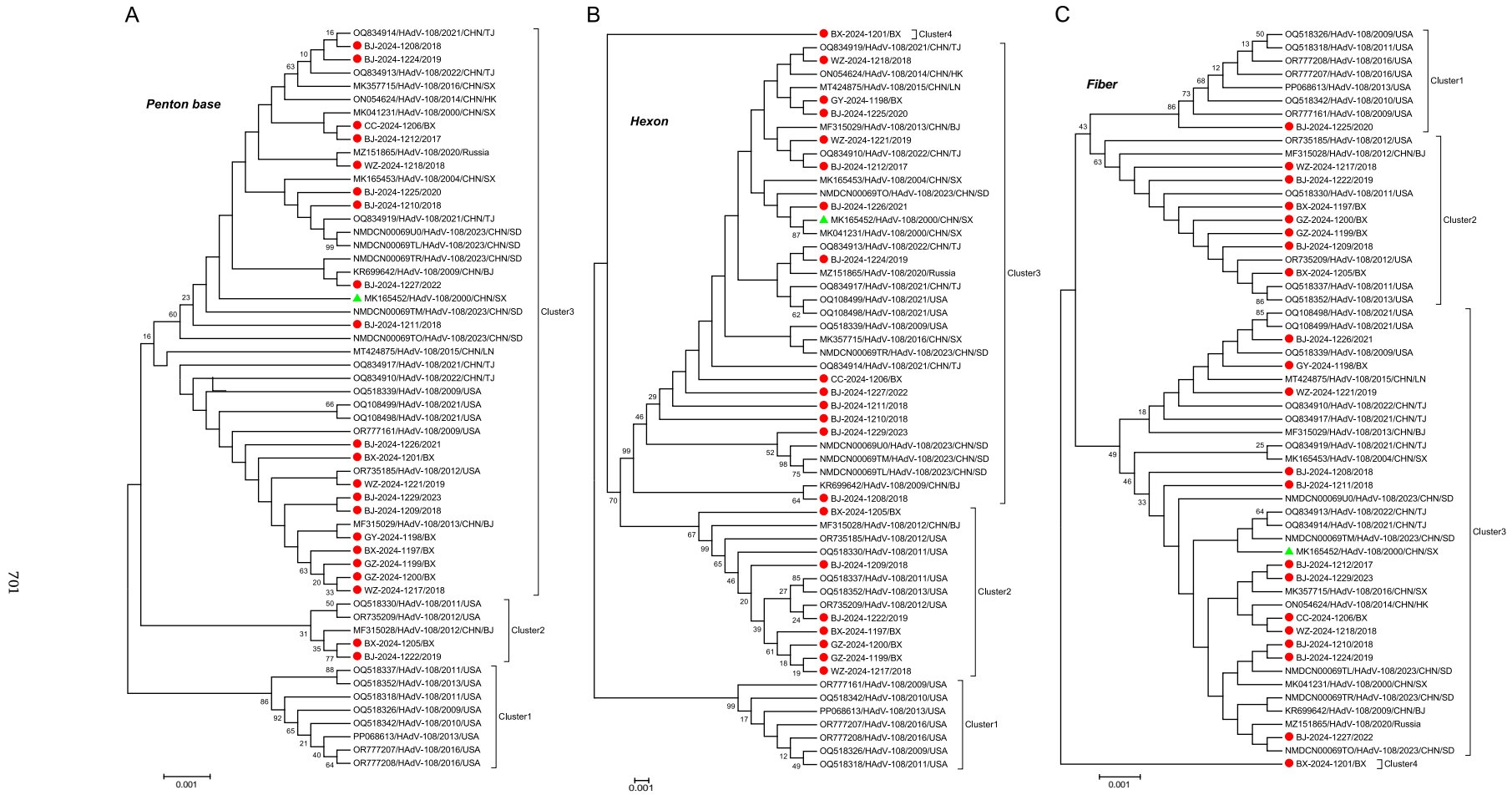
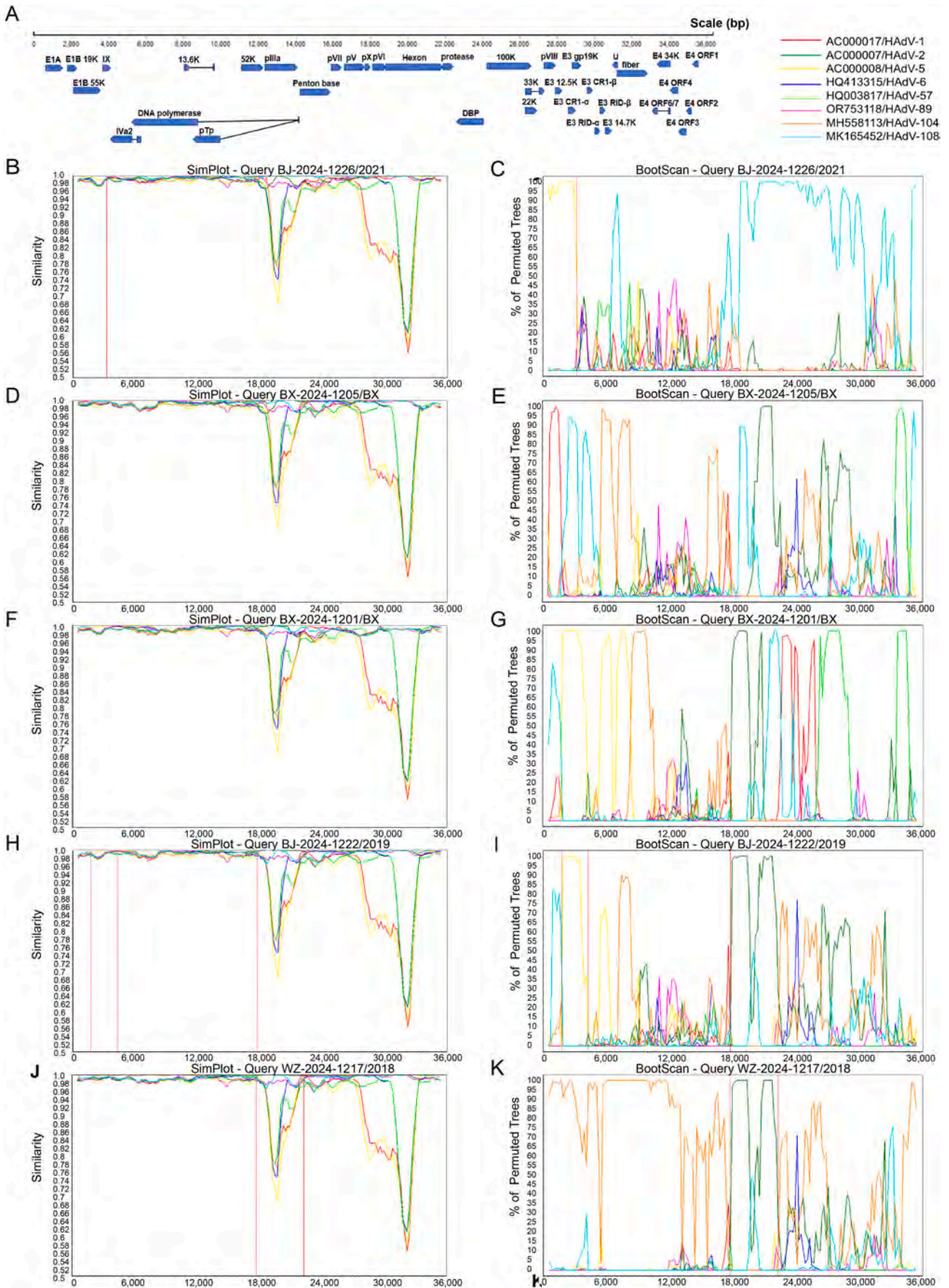


Fig. 4. Phylogenetic analysis of three major capsid protein genes of HAdV-108. The phylogenetic tree of *penton base* gene (A) was constructed by the Maximum Likelihood method and the Tamura 3-parameter model using 1000 replicates. The phylogenetic tree of *hexon* gene (B) was constructed by the Maximum Likelihood method and the Kimura 2-parameter model using 1000 replicates. The phylogenetic tree of *Fiber* gene (C) was constructed by the Maximum Likelihood method and the Hasegawa-Kishino-Yano model using 1000 replicates. Cyan triangle indicates the SX-2000-140 strain (the earliest reported strain of HAdV-108, GenBank accession number: MK165452). Strains obtained in this study are indicated by red dots.



(caption on next page)

Fig. 6. Representation of 5 recombination patterns in 21 HAdV-108 genomes obtained in this study. **A** Genetic organization of HAdV-108. SimPlot (**B**) and BootScan (**C**) analysis of the whole genome of the BJ-2024-1226/2021 strain. The WZ-2024-1221/2019 and BJ-2024-1226/2021 strains had the same recombination pattern. Therefore, the BJ-2024-1226/2021 strain was selected as the representative to display the results of recombination analysis. SimPlot (**D**) and BootScan (**E**) analysis of the whole genome of the BX-2024-1205/BX strain. SimPlot (**F**) and BootScan (**G**) analysis of the whole genome of the BX-2024-1201/BX strain. SimPlot (**H**) and BootScan (**I**) analysis of the whole genome of the BJ-2024-1222/2019 strain. SimPlot (**J**) and BootScan (**K**) analysis of the whole genome of the WZ-2024-1217/2018 strain. Because the BX-2024-1197/BX, GZ-2024-1199/BX, GZ-2024-1200/BX, BJ-2024-1209/2018, and WZ-2024-1217/2018 strains had the same recombination pattern, the WZ-2024-1217/2018 strain was selected as the representative to display the results of recombination analysis.

A homology model of penton base protein of the GZ-2024-1200/BX strain was built and superimposed with that of the SX-2000-140 strain to visualize the structural variations (Fig. 5B). The root mean square deviation (RMSD) for the two superimposed structures was 0.012. Upon alignment, disparities were observed at the amino acid deletion sites of the RGD loop region. However, the impact of these variations on functionality necessitates further study. Selection pressure analysis showed that penton base protein contained a positive selection site 47, where a change occurred from hydrophilic basic amino acid (R) to nonpolar hydrophobic amino acid (A). This amino acid substitution was exclusively observed in two strains isolated from Shandong, China in 2023 (NMDC accession numbers: NMDCN00069U0 and NMDCN00069TL). No negative selection site was found. Homology models of fiber protein of the SX-2000-140, BX-2024-1201/BX and BJ-2024-1227/2022 strains were built, and the mutation sites were marked on the models. Alignment of the three fiber model structures revealed no distinct differences at the amino acid mutation sites of the Knob region (Fig. 5C and D). Selection pressure analysis showed that no positive or negative selection site was found in fiber protein.

In addition, the amino acid variation analysis indicated that, apart from the three major capsid proteins mentioned above, mutations predominantly occurred in proteins encoded by early genes, particularly the E1 and E2 regions. Other proteins primarily exhibited sporadic mutations (Fig. 5E).

Recombination analysis

According to the recombination analysis, five distinct recombination patterns were identified in the 21 whole genome sequences of HAdV-108 obtained in this study (Fig. 6). The first recombination pattern revealed that the genome skeleton of the WZ-2024-1221/2019 and BJ-2024-1226/2021 strains derived from HAdV-108, with the *E1A*, *E1B* 19 kDa protein and a segment of *E1B* 55 kDa protein genes (approximately nt0-3197) originating from HAdV-5 (Fig. 6B and C). The second and third recombination patterns, the BX-2024-1205/BX and BX-2024-1201/BX strains, were both products of homologous recombination involving HAdV-1, -2, -57, -104 and -108 at different positions (Fig. 6D–G). The fourth recombination pattern showed that the BJ-2024-1222/2019 strain was a recombinant of HAdV-2, -5 and -104, with the breakpoint identified around position 17843. HAdV-104 served as the backbone of the first half, with the *E1B* and hexon-associated protein IX genes embedded with HAdV-5, while the second half used HAdV-2 as the

backbone (Fig. 6H and I). The five strains (BX-2024-1197/BX, GZ-2024-1199/BX, GZ-2024-1200/BX, BJ-2024-1209/2018, and WZ-2024-1217/2018) shared an identical recombination pattern, using HAdV-104 as the backbone. A recombination event involving HAdV-2 at nt17812-22372 were observed, including partial sequences of protein X precursor, protein VI precursor, *hexon*, and protease genes (Fig. 6J and K). The remaining strains displayed high similarity ($\geq 98.5\%$) with the SX-2000-140 strain, located in the same phylogenetic branch, and no new recombination events were detected.

Analysis of divergence time and evolution rate

Through calculation, HAdV-108 exhibited the highest nucleotide sequence identity with HAdV-2 (Table 3). Bayesian evolutionary analysis based on the whole genome sequences showed that HAdV-108 diverged around 1635 (95% of the highest posterior density (HPD) in 1294–1922) (Table 4). Cluster2 and Cluster3 appeared approximately in 1735 (Fig. 7). The molecular evolution rate of HAdV-108 whole genomes was about 2.21×10^{-5} substitutions/site/year (95% HPD, 8.3×10^{-6} – 4.47×10^{-5} substitutions/site/year). As shown in Table 4, among the three major capsid protein genes, *hexon* had the fastest evolution rate, while *fiber* had the earliest divergence time but the slowest evolution rate. The Maximum Clade Credibility (MCC) trees with estimated divergence time of *penton base*, *hexon*, and *fiber* genes of HAdV-108 are shown in Supplementary Fig. S1.

Comparative analysis of the proliferation of HAdV-108 with other types of species C

All strains of species C were able to effectively proliferate in A549 cells. The virus titer began to increase significantly 12 h post-infection and continued to rise, though the curve gradually flattened. Distinct cytopathic effects (CPE) were observed in cells 72 h after infection with different strains (Fig. 8B–E and Supplementary Fig. S2). HAdV-108 had comparable virus titer and CPE to other types within species C, with no statistically significant differences observed in the replication dynamics ($P > 0.05$) (Fig. 8A).

DISCUSSION

This study is the most comprehensive investigation in China on HAdV-108-associated acute respiratory tract infection in children, with

Table 3

The nucleotide sequence identities between HAdV-108 and representative strains of other types of species C.^a

	HAdV-1	HAdV-2	HAdV-5	HAdV-6	HAdV-57	HAdV-89	HAdV-104
Nucleotide identity	92%–94.7%	96.5%–99.5%	91.3%–93.9%	94%–96.8%	93.3%–96%	96.3%–99.4%	95.4%–98.4%

Note: ^a Representative strains of other types within species C are showed in Supplementary Table S3.

Table 4

The estimated divergence time and evolutionary rates of the whole genome and three major capsid protein genes of HAdV-108.

	Whole genome	Penton base	Hexon	Fiber
Divergence time/year (95% HPD ^a)	1635 [1294, 1922]	1970 [1888, 2000]	1960 [1861, 2000]	1883 [1588, 2000]
Evolution rate/ 10^{-5} substitutions/site/year (95% HPD)	2.21 [0.83, 4.47]	7.80 [1.29, 15.89]	24.64 [5.72, 43.87]	3.25 [0.16, 7.68]

Note: ^a 95% HPD: 95% of the highest posterior density.

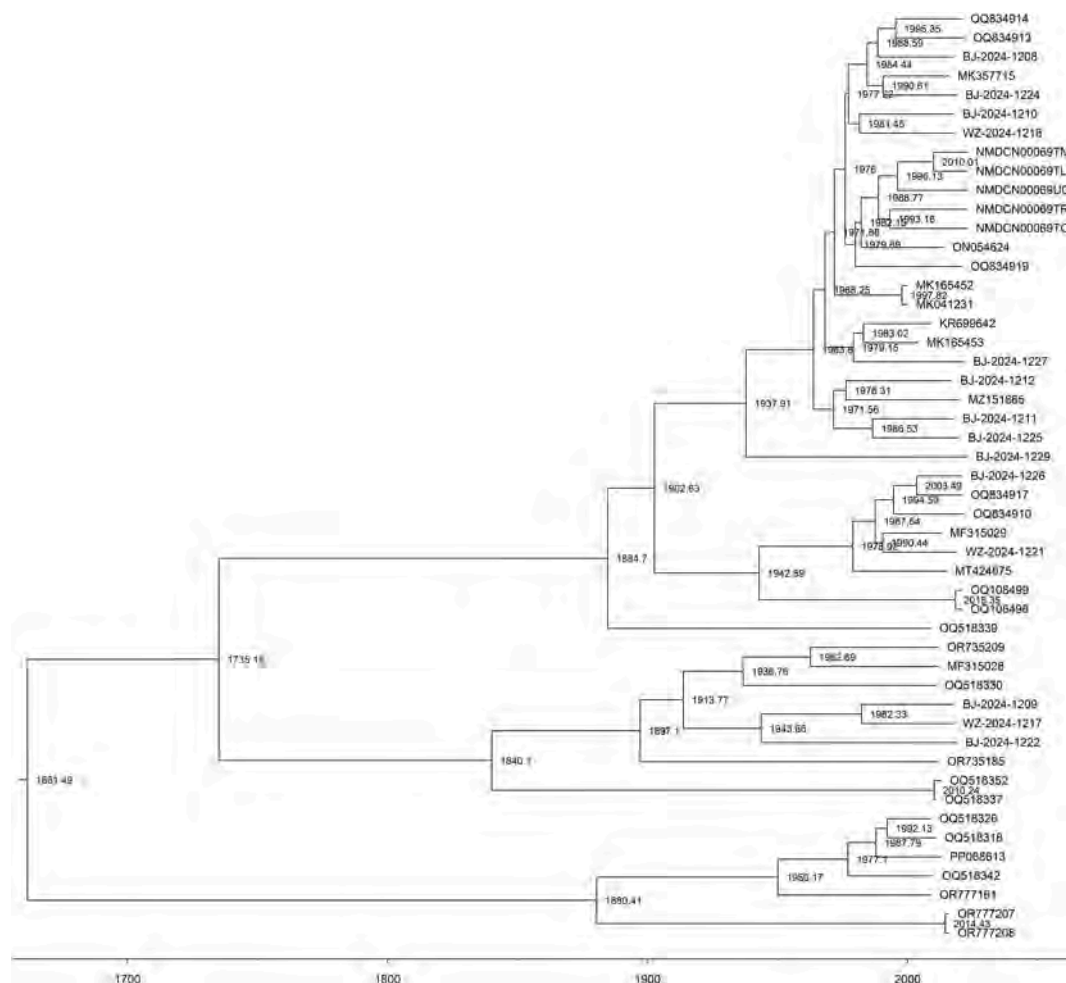


Fig. 7. The Maximum Clade Credibility tree with estimated divergence time of HAdV-108 whole genome sequences. The tick mark represents the year.

the widest geographic coverage and the largest number of participating study centers to date. Furthermore, it is also the first systematic study focusing on HAdV-108 infection and genetic variation in children since its identification as a novel type in 2014. In this prospective multicenter study, 21 HAdV-108-positive samples were identified during the study period, accounting for 6.62% of all successfully isolated HAdV-positive samples and ranking third after HAdV-114 and -7. Cough and fever were the primary manifestations in children with HAdV-108 infection, with seven children presenting gastrointestinal symptoms. Notably, two children without underlying diseases were diagnosed with severe pneumonia. No significant differences were observed in the overall clinical characteristics among children infected with HAdV-1/2 or 108. Previous studies have reported varying detection rates of HAdV-108 in China, with an observed correlation with severe illnesses in children. Wang et al. found that P1H2F2 constituted approximately 4.7% of all HAdV-positive samples from children hospitalized with severe ARI in three provinces across northern and southern China between September 2007 and March 2014 (Wang et al., 2016). Cai et al. identified HAdV-108 in 9.8% of HAdV-positive throat swab samples from hospitalized children with severe ARI in eight provinces of northern and southern China between 2017 and 2021, ranking fourth after HAdV-1, -3, and -7 (Cai et al., 2024). Cheng reported that from January to August 2021, 18.9% of HAdV-positive throat swabs from outpatient children under 16 years diagnosed with ARI and screened negative for influenza virus in Wuwei, Gansu, China were identified as HAdV-108 (Cheng, 2024). Wu et al. found that the detection rate of HAdV-108 was 7.33% among all HAdV-positive samples from children hospitalized with ARI in Wuhan from 2022 to 2023, ranking second only to

HAdV-3. Patients infected with HAdV-1, -2, -5, -104 and -108 exhibited similar clinical manifestations, mainly fever and cough. It is noteworthy that 36.36% of children infected with HAdV-108 developed sepsis (Wu et al., 2025). The differences in detection rates of HAdV-108 may be attributed to various factors, including the number of research centers, research areas, detection methods, inclusion/exclusion criteria, sample size, the age of the patients, sample source and collection time, duration of the research, the prevalence of adenovirus at that time, among others. Nonetheless, these findings consistently emphasize that HAdV-108 persists in circulation in China, causing ARI and even severe ARI in pediatric patients—underscoring the critical need for enhanced awareness and monitoring. Abroad, HAdV-108 infections were primarily sporadic (Kurskaya et al., 2024), though fatal cases have been documented (Becken et al., 2024).

The phylogenetic tree of the HAdV-108 whole genome sequences revealed four evolutionary branches. Cluster1 and Cluster2 were the predominant epidemic branches abroad in the early years. Among the strains from China, no strains fell within Cluster1. Only the BJ04 strain (GenBank accession number: MF315028) found in Beijing in 2012 and a few of the sequences obtained in this study were located in Cluster2. Cluster3 was the dominant epidemic lineage in China, with sporadic occurrences in USA and Russia in recent years. All strains identified worldwide from 2020 onwards belonged to Cluster3. One stain obtained in this study, the BX-2024-1201/BX strain, independently formed an evolutionary branch, Cluster4. These findings suggest that with the development of society and economy, the frequent movement of populations between countries may facilitate the cross-spread of different epidemic branches in different regions. However, whether Cluster3 will

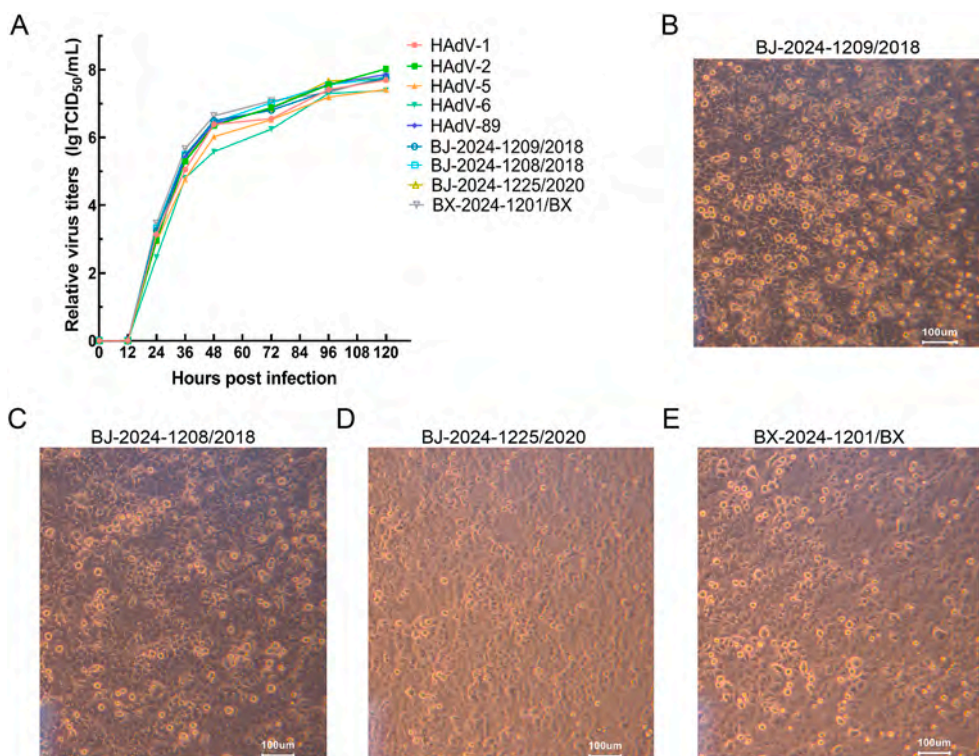


Fig. 8. Comparative analysis of the replication dynamics of HAdV-108 with other types of species C. A Growth kinetics of species C at 0, 12, 24, 36, 48, 72, 96 and 120 h post-infection in A549 cells; $n = 3$. Cytopathic effects in cells 72 h after the BJ-2024-1209/2018 (B), BJ-2024-1208/2018 (C), BJ-2024-1225/2020 (D), and BX-2024-1201/BX (E) strains infections.

replace Cluster1 and Cluster2 as the predominant epidemic branch abroad, or whether Cluster4 independently formed by the BX-2024-1201/BX strain obtained in this study will become a new epidemic branch in the future, remains uncertain. Continuous surveillance of the prevalence of HAdV-108, along with comprehensive whole genome sequencing and analysis, is still necessary. Through calculation, it was found that HAdV-108 shared the highest nucleotide sequence identity with HAdV-2, hinting at a common ancestry between the two viruses, in line with prior studies (Yang et al., 2019). According to the analysis of divergence time, it was estimated that HAdV-108 diverged from the common ancestor with HAdV-2 around 1635. Subsequently, Cluster2 and Cluster3 appeared around 1735. However, due to the limited whole genome sequences of HAdV-108 with collection time, the results may have some potential bias and are for reference only. Historically, serotyping relied on serum neutralization and hemagglutination inhibition tests by detecting antigenic epitopes in hexon and fiber proteins, leading to misclassification of HAdV-108 as HAdV-2 due to similarities in *hexon* and *fiber* coding regions (Lynch and Kajon, 2021). Considering the possibility of wrong typing, as of December 31, 2024, the sequences that may be considered as HAdV-108 but are registered as HAdV-2 in GenBank were examined by BLAST and phylogenetic analyses. The results revealed that several sequences classified as HAdV-2 from Germany (GenBank accession numbers: MH121079, MH121078, MH121099, MH121095), the United Kingdom (GenBank accession number: MW686842), and China (GenBank accession numbers: MK883607, MK883605, MK905735), among others, exhibited high similarity to HAdV-108 ($\geq 97\%$). Their penton base genes belonged to HAdV-1, while the hexon and fiber genes belonged to HAdV-2. Therefore, despite the limited availability of HAdV-108 sequences, the geographic diversity of the similar sequences suggested potential global circulation of HAdV-108. To better comprehend the prevalence of HAdV-108 in populations, more accurate epidemiological data are essential.

In comparison with the earliest HAdV-108 strain identified to date, the SX-2000-140 strain (GenBank accession number: MK165452), the

HAdV-108 strains obtained in this study had amino acid mutations in the RGD loop region of penton base protein and the Knob region of fiber protein. Hexon protein exhibited the most cluster-specific amino acid mutations, followed by penton base protein. In contrast, fiber protein showed the highest degree of conservation. These findings suggested that changes of epitopes related to immune escape were more likely to occur in hexon, consistent with the most previous studies on other HAdVs (Liu et al., 2021, 2023). Compared with previously described HAdV-C strains, HAdV-108 displayed significant diversity in penton base protein, which not only exhibited cluster-specific amino acid mutations, but also had three new amino acid deletions in the strains obtained in this study and isolated from Shandong, China in 2023 (NMDC accession numbers: NMDCN00069TO, NMDCN00069TR, NMD CN00069U0, NMDCN00069TL, and NMDCN00069TM). Protein structure modeling revealed that these deletions resulted in structural differences in penton base protein, which might impact the binding to integrins on the host cell surface and thereby affecting the viral entry process (Hofmayer et al., 2009). Further research is needed to clarify the functional significance of these mutations. Selection pressure analysis indicated a positive selection site 47 in penton base protein of HAdV-108, involving a transition from hydrophilic basic amino acid (R) to nonpolar hydrophobic amino acid (A). Conversely, hexon protein contained a negative selection site 763 (K). Since both sites were located outside the primary functional regions of the respective proteins, with the former observed only in two strains isolated from Shandong, China in 2023 (NMDC accession numbers: NMDCN00069U0 and NMDCN00069TL), the functional implications of these two positive and negative selection sites remain an open question and require further investigation.

Among the three major capsid protein genes, *fiber* gene exhibited the earliest divergence time but the slowest evolution rate (3.25×10^{-5} substitutions/site/year), while *hexon* gene displayed the fastest evolution rate (2.46×10^{-4} substitutions/site/year), closed to that of HAdV-3 (2.34×10^{-4} substitutions/site/year) in species B (Lin et al., 2015),

higher than that of HAdV-4 (1.86×10^{-5} substitutions/site/year) in species E (Li et al., 2018), HAdV-31 (approximately 2×10^{-5} substitutions/site/year) in species A (Liu et al., 2023), and HAdV-41 (about 6×10^{-5} substitutions/site/year) in species F (Liu et al., 2021), but lower than that of HAdV-7 (1.107×10^{-3} substitutions/site/year) in species B (Lin et al., 2015). These results were in line with the findings of the amino acid variation analysis, indicating the pivotal involvement of the *hexon* gene in the evolution of HAdV-108. Apart from the three major capsid proteins, amino acid mutations were mainly observed in proteins encoded by early genes, especially the E1 and E2 regions, suggesting that these regions may also play a crucial role in evolution and immune evasion of HAdV-108, which needs further study.

Recombination is a well-established characteristic of HAdV genetics and a key factor driving HAdV evolution (Walsh et al., 2009). Previous studies have demonstrated that HAdV-108 was a product of interspecific recombinant, inheriting the *penton base* gene from HAdV-1 and the *hexon* and *fiber* genes from HAdV-2 (Wang et al., 2024). Therefore, it was plausible to assume that the tropism of HAdV-108 resembled that of HAdV-1 and HAdV-2 (Yang et al., 2019), offering an explanation for the gastrointestinal manifestations observed in certain individuals in this study. Recombination analysis of the whole genome sequences of the 21 HAdV-108 strains obtained in this study revealed five distinct recombination patterns involving multiple types belonging to species C, with recombination events occurring at various locations. The emergence of various recombination patterns may be related to the progressive accumulation of natural variation and recombination events during evolution (Yang et al., 2019). Additionally, it also reflects the diverse genetic recombination of HAdV-108 (Cheng, 2024), consistent with the considerable diversity observed in the epidemic strains of species C (Lei et al., 2023). Previous studies have also reported that the genome evolutionary diversity among different sequences of HAdV-108 isolates was inconsistent, with substantial intra-type genetic variability (Dhingra et al., 2019; Becken et al., 2024), and potential recombination events occurred at multiple genomic sites in a random and diverse manner (Wang et al., 2016; Cheng, 2024; Lei et al., 2023). Some analyses indicated that the differences among the prototype strains of species C were primarily concentrated in the three major capsid protein genes, suggesting that the recombination events in other genome regions may have limited biological significance. However, describing recombination events can indirectly assist in identifying viruses circulating at specific locations and times, facilitating the understanding of viral replacement rates, which is crucial for the monitoring, prevention and control of HAdVs (Lei et al., 2023; Mao et al., 2017). Hence, it is imperative to maintain active surveillance of HAdV-108.

In vitro experiments showed that the replication dynamics of HAdV-108 closely resembled those of its parental strains, HAdV-1 and -2. Ji et al. found that the plaque sizes formed by PH2F2 were similar to those generated by HAdV-1, -2, and -104, suggesting a potential equivalence in virulence among these types in cultured cells (Ji et al., 2021). Kurskaya et al. observed comparable viral titers for HAdV-1, -2, -5, -89, and -108, indicating no significant disparities in viral growth among these types (Kurskaya et al., 2024). Any emerging recombinant adenovirus strains may pose unforeseen risks, including severe outbreaks in dense populations, which in turn can lead to high morbidity and mortality, particularly among immunocompromised patients susceptible to HAdV-C (Dhingra et al., 2019; Ji et al., 2021; Mao et al., 2019). Therefore, ongoing monitoring of the recently confirmed novel type, HAdV-108, is crucial.

This study also had some limitations. First, although the samples were collected from ten hospitals across northern and southern China, the vast geographic diversity of China restricted the representativeness of the findings in the study. Second, this study exclusively focused on hospitalized children with ARIs, and the detection of HAdV-108-positive samples was constrained in number. Furthermore, the clinical data were unavailable for some samples that only had genome sequences, making the clinical and genetic variation characteristics primarily reference.

CONCLUSIONS

This multicenter study showed that HAdV-108, an interspecies genetic recombinant of two common HAdV types, persistently circulated in China, underscoring the importance of continued monitoring of its genetic changes and associated impacts. ARI associated with HAdV-108 might be severe and manifest with concomitant gastrointestinal symptoms. According to whole genome sequences available, HAdV-108 can currently be divided into four phylogenetic branches, and Cluster3 is identified as the predominant epidemic branch in China. Among the three major capsid proteins, hexon exhibited the fastest evolution rate, the lowest sequence identity, and the highest amino acid variability. In contrast, fiber protein displayed the slowest evolution rate, the highest identity, and the greatest conservation and stability. New amino acid deletions were found in the RGD loop region of penton base protein, leading to potential structural change, but the biological significance needs further investigation. HAdV-108 exhibited considerable intra-type genetic variation, with random and diverse recombination events, and its proliferation capacity was comparable to that of other types within species C, including HAdV-1 and -2. This study further clarified the clinical and genetic characteristics of HAdV-108 circulating in China and provided a reference for the surveillance, prevention and control of HAdV-108, as well as the research and development of vaccines and drugs.

MATERIALS AND METHODS

Patients and clinical data collection

Children under 18 years hospitalized for ARIs in ten hospitals across nine regions in China (Guangzhou Women and Children's Medical Center, Yinchuan Women and Children Healthcare Hospital, the 2nd Affiliated Hospital and Yuying Children's Hospital of Wenzhou Medical University, Guiyang Maternal and Child Health Hospital, Shengjing Hospital of China Medical University, Xin Hua Hospital Affiliated to Shanghai Jiao Tong University School of Medicine, Children's Hospital of Hebei Province, Children's Hospital of Changchun, The Children's Hospital, Zhejiang University School of Medicine, and Beijing Children's Hospital, Capital Medical University) from 2014 to 2024 were included in this prospective multicenter study. All of these hospitals are tertiary grade A hospitals and have specialized pediatric departments. Children with a disease course longer than seven days or whose parents or guardians disagreed were excluded. The clinical data were collected through the clinical electronic medical record system.

Specimen collection and HAdV detection

Respiratory samples, including sputum, nasal/pharyngeal swabs, bronchial lavage fluid, and nasopharyngeal aspirates, were collected within 24 h post-admission, then transported to various hospital laboratories for processing at 4 °C. Following this, the samples were stored in the –80 °C refrigerator and conveyed to virology laboratory of the Beijing Children's Hospital affiliated to Capital Medical University using dry ice for centralized detection and analysis. The viral nucleic acids were extracted using the QIAamp MinElute Virus Spin Kit (QIAGEN, Germany) as per the manufacturer's protocols. The common respiratory viruses, including enterovirus, human rhinovirus, respiratory syncytial virus, parainfluenza virus, HAdV, coronavirus, influenza virus, bocavirus and human metapneumovirus, were detected using the Multiple Respiratory Virus Panel (Luminex Corporation, USA).

Virus isolation and sequencing of whole genome

Following inoculation of HAdV-positive samples into Hep-2 or A549 cells purchased from American type culture collection (ATCC) for virus isolation, the nucleic acids of the isolated HAdV strains were

submitted to Annaroad Gene Technology Co., Ltd (Beijing, China) for whole genome sequencing via Illumina sequencing platform. The whole genome sequences were annotated utilizing Prokka v1.11 and then uploaded to the GenBank database.

HAdV typing

The *penton base*, *hexon*, and *fiber* gene sequences were extracted from the whole genome sequences of HAdV obtained above. The typing was preliminarily determined by aligning these three major capsid protein gene sequences with those in GenBank using BLAST. The reference sequences of *penton base*, *hexon*, and *fiber* genes of HAdV worldwide were chosen from the GenBank database, excluding those showing significant consistency in region, time and sequence. MAFFT (<https://www.ebi.ac.uk/Tools/msa/mafft/>) software was used for multiple alignments of the three major capsid protein gene sequences. MEGA v7.0.26 (Sudhir Kumar, Arizona State University, Tempe, AZ, United States) software was used to construct the phylogenetic trees through the Neighbor-Joining method and Kimura 2-parameter model with a bootstrap test of 1000 replicates to further determine the typing.

Phylogenetic analysis

The GenBank database and China NMDC were used to select the reference sequences of the whole genome, *penton base*, *hexon*, and *fiber* genes of HAdV-108 for phylogenetic analysis. Similarly, MAFFT (<https://www.ebi.ac.uk/Tools/msa/mafft/>) software was used for multiple alignments of the whole genome, *penton base*, *hexon*, and *fiber* gene sequences. The phylogenetic trees were constructed using MEGA v7.0.26 (Sudhir Kumar, Arizona State University, Tempe, AZ, United States) software through the Maximum Likelihood method with 1000 bootstrap replicates. The optimal model for tree construction was determined based on the lowest Bayesian Information Criterion score.

Genetic variation analysis

The genetic variations of the genes and proteins of HAdV-108 were determined using BioEdit v7.2.05 software (<http://www.mbio.ncsu.edu/BioEdit/page2.html>). Homology models of the proteins were built by Python v3.10.7 and Swiss-Model ExPASy. Hyphy v2.5.8 was used for selective pressure analysis. Five algorithms were applied to identify negative (purifying) and positive (diversifying) selection at the codon level: single-likelihood ancestor counting method, fixed-effects likelihood, mixed-effects model of evolution, fast unconstrained bayesian application, and branch-site unrestricted statistical test for episodic diversification. Positive selections were inferred with a *P*-value <0.1 or a posterior probability >0.9 for a minimum of two of the aforementioned methods, while negative selections were inferred with a *P*-value <0.05 or a posterior probability >0.95 for a minimum of two of the aforementioned methods.

Recombination analysis

Simplot v3.5.1 software was used for recombination analysis of the HAdV-108 whole-genomic sequences obtained in this study. The parameters were set to window size 1000, step size 200, gap stripping turned on and Kimura (two parameter) distance correction.

Analysis of divergence time and evolution rate

BEAST v10.5.0 was used to estimate the divergence time and evolution rate (substitutions/site/year) with the Markov chain Monte Carlo method. The best-fit nucleotide substitution model was generated in PhyloSuite v1.2.3: model HKY + F + G4. The uncorrelated log-normal relaxed clock was the optimal model for evolutionary computation. Tracer v1.7.2 was used to assess the quality of the posterior distribution

of each setting according to the effective sample size with 10% burning. The MCC trees with divergence time were constructed using FigTree v1.4.4.

Viral growth kinetics

Other types strains of species C (HAdV-1, -2, -5, -6, -89) previously stored in our laboratory and the HAdV-108 strains obtained in this study, which were located in different phylogenetic branches of the whole genome sequence phylogenetic tree and associated with severe infections, were used to infect A549 cells at 80% confluency in 96-well plates with a multiplicity of infection (MOI) of 0.1. After 2h adsorption, the inoculum was removed and the maintenance media (Dulbecco's Modified Eagle Medium+2% fetal bovine serum+1% Penicillin-Streptomycin solution) was added to each well. The plates were then incubated at 37 °C in 5% CO₂. Cells and supernatant were harvested at 0, 12, 24, 36, 48, 72, 96 and 120 h post-infection. Tissue culture infective dose 50% (TCID₅₀) was used to titer the virus at each time point. GraphPad Prism v9.5.1 and SPSS v27.0 were used for the statistical analyses. The Mann-Whitney U tests and Bonferroni test were applied to calculate the differences between groups. *P*-values <0.05 were considered statistically significant.

Statistical analysis

The analyses were performed using SPSS v27.0. Count data were described as cases (%). The chi-square (χ^2) test and one-way analysis of variance were used to compare differences between groups. Differences were considered statistically significant at *P*-values <0.05.

DATA AVAILABILITY

All data generated or analyzed during this study are included in this published article (and its supplemental files). The sequences generated in this study were submitted to the GenBank database in the National Center for Biotechnology Information (NCBI, <https://www.ncbi.nlm.nih.gov/>) and Science Data Bank (<https://doi.org/10.57760/sciencedb.24156>). The accession numbers are listed in Supplementary Table S1.

ETHICS STATEMENT

This study was approved by the Institutional Ethics and Review Committees of the Beijing Children's Hospital affiliated to Capital Medical University ([2023]-E-171-Y, 2019-k-357) and conducted in accordance with Helsinki Declaration (revised in 2013). Parents or legal-guardians of children included in this study all agreed and signed written informed consents.

AUTHOR CONTRIBUTIONS

Jinjin Wang: conceptualization, data curation, formal analysis, investigation, methodology, validation, visualization, writing-original draft, writing - review & editing. Ling Jing: data curation, formal analysis, investigation, methodology, validation, visualization. Yali Duan: data curation, formal analysis, investigation, methodology. Junhong Ai: formal analysis, investigation, methodology. Yun Zhu: data curation, formal analysis, investigation, methodology. Ran Wang: formal analysis, investigation, methodology. Xiangpeng Chen: formal analysis, investigation, methodology. Gen Lu: data curation, resources. Yun Sun: data curation, resources. Changchong Li: data curation, resources. Rong Jin: data curation, resources. Yunxiao Shang: data curation, resources. Yixiao Bao: data curation, resources. Shuhua An: data curation, resources. Yunlian Zhou: data curation, resources. Limin Ning: data curation, resources. Baoping Xu: data curation, resources. Yuhai Bi: methodology. Zhengde Xie: conceptualization, formal analysis, funding acquisition,

methodology, project administration, resources, supervision, validation, visualization, writing-review & editing.

CONFLICT OF INTEREST

The authors declare that they have no conflict of interest. Prof. Zhengde Xie and Prof. Yuhai Bi are editorial board members for *Virologica Sinica* and were not involved in the editorial review or the decision to publish this article.

ACKNOWLEDGEMENTS

This work was supported by National Key Research and Development Program of China (2023YFC2306001), National Natural Science Foundation of China (No.32470141), the Beijing Research Center for Respiratory Infectious Diseases Project (BJRID2025-008) and CAMS Innovation Fund for Medical Sciences (CIFMS, NO.2019-I2M-5-026, 2022-I2M-CoV19-006). We would like to express our sincere appreciation to our institutes and universities.

APPENDIX A. SUPPLEMENTARY DATA

Supplementary data to this article can be found online at <https://doi.org/10.1016/j.virs.2025.09.002>.

REFERENCES

- Becken, B.A., Lamson, D.M., Gonzalez, G., Patel, S., St George, K., Kajon, A.E., 2024. A fulminant case of adenovirus genotype C108 infection in a pediatric stem cell transplant recipient with x-Linked lymphoproliferative syndrome type 1. *Viruses* 16, 137.
- Bezerra, P.G., Britto, M.C., Correia, J.B., Duarte Mdo, C., Fonseca, A.M., Rose, K., Hopkins, M.J., Cuevas, L.E., McNamara, P.S., 2011. Viral and atypical bacterial detection in acute respiratory infection in children under five years. *PLoS One* 6, e18928.
- Cai, J., Liu, Y., Qian, C., Gao, Y., Zhao, S., Ma, Y., Xiang, X., Xu, J., Zhang, F., Li, M., Xu, H., Li, Q., Li, C., Lin, Y., Xia, B., Cui, A., Zhang, Y., Zhu, Z., Mao, N., 2024. Genetic characterization of pediatric SARI-Associated human adenoviruses in eight Chinese provinces during 2017–2021. *J. Med. Virol.* 96, e29618.
- Cheng, Q., 2024. Analysis of the pathogenic spectrum of patients with acute respiratory tract infections and molecular epidemiological characterization of human adenovirus in wuwei, Gansu Province, 2021. AUST, MA thesis. <https://doi.org/10.26918/d.cnki.gnhgc.2024.001326> (in Chinese).
- Davison, A.J., Benko, M., Harrach, B., 2003. Genetic content and evolution of adenoviruses. *J. Gen. Virol.* 84, 2895–2908.
- Dhingra, A., Hage, E., Ganzenmueller, T., Bottcher, S., Hofmann, J., Hamprecht, K., Obermeier, P., Rath, B., Hausmann, F., Dobner, T., Heim, A., 2019. Molecular evolution of Human Adenovirus (HAdV) species C. *Sci. Rep.* 9, 1039.
- Hofmayer, S., Madisch, I., Darr, S., Rehren, F., Heim, A., 2009. Unique sequence features of the Human adenovirus 31 complete genomic sequence are conserved in clinical isolates. *BMC Genom.* 10, 557.
- Huang, S., Wang, H., Li, L., Xiang, W., Song, Z., Li, W., 2023. Molecular epidemiology and phylogenetic analyses of human adenovirus in pediatric patients with acute respiratory infections from Hangzhou during COVID-19 pandemic. *Front Pediatr* 11, 1237074.
- Ismail, A.M., Cui, T., Dommaraju, K., Singh, G., Dehghan, S., Seto, J., Shrivastava, S., Fedorova, N.B., Gupta, N., Stockwell, T.B., Halpin, R., Madupu, R., Heim, A., Kajon, A.E., Romanowski, E.G., Kowalski, R.P., Malathi, J., Therese, K.L., Madhavan, H.N., Zhang, Q., Ferreyra, L.J., Jones, M.S., Rajaiya, J., Dyer, D.W., Chodosh, J., Seto, D., 2018. Genomic analysis of a large set of currently-and historically-important human adenovirus pathogens. *Emerg. Microb. Infect.* 7, 10.
- Ji, T., Li, L., Li, W., Zheng, X., Ye, X., Chen, H., Zhou, Q., Jia, H., Chen, B., Lin, Z., Chen, H., Huang, S., Seto, D., Chen, L., Feng, L., 2021. Emergence and characterization of a putative novel human adenovirus recombinant HAdV-C104 causing pneumonia in Southern China. *Virus Evol.* 7, veab018.
- Kurskaya, O.G., Prokopyeva, E.A., Dubovitskiy, N.A., Solomatina, M.V., Sobolev, I.A., Derko, A.A., Nokhova, A.R., Anoshina, A.V., Leonova, N.V., Simkina, O.A., Komissarova, T.V., Tupikin, A.E., Kabilov, M.R., Shestopalov, A.M., Sharshov, K.A., 2024. Genetic diversity of the Human adenovirus C isolated from hospitalized children in Russia (2019–2022). *Viruses* 16, 386.
- Lei, Y., Zhuang, Z., Liu, Y., Tan, Z., Gao, X., Li, X., Yang, D., 2023. Whole genomic sequence analysis of human adenovirus species C shows frequent recombination in tianjin, China. *Viruses* 15, 1004.
- Li, H., Mao, N.Y., Yu, P.B., Yin, J., Jiang, H.B., Zhang, B., Meng, T.Y., Sun, L.W., Cui, A.L., Xu, W.B., Zhu, Z., Zhang, R.B., 2018. Genetic characteristics of human adenovirus type 4 in acute respiratory tract infection in four provinces of China from 2013 to 2014. *Chin. J. Virol.* 34, 850–859 (in Chinese).
- Lin, Y.C., Lu, P.L., Lin, K.H., Chu, P.Y., Wang, C.F., Lin, J.H., Liu, H.F., 2015. Molecular epidemiology and phylogenetic analysis of human adenovirus caused an outbreak in Taiwan during 2011. *PLoS One* 10, e0127377.
- Liu, L., Qian, Y., Han, Z., Jia, L., Dong, H., Zhao, L., Zhu, R., 2023. Genetic evolution and variation of human adenovirus serotype 31 epidemic strains in Beijing, China, during 2010–2022. *Viruses* 15, 1240.
- Liu, L., Qian, Y., Jia, L., Dong, H., Deng, L., Huang, H., Zhao, L., Zhu, R., 2021. Genetic diversity and molecular evolution of human adenovirus serotype 41 strains circulating in Beijing, China, during 2010–2019. *Infect. Genet. Evol.* 95, 105056.
- Lynch 3rd, J.P., Kajon, A.E., 2021. Adenovirus: epidemiology, global spread of novel types, and approach to treatment. *Semin. Respir. Crit. Care Med.* 42, 800–821.
- Madisch, I., Harste, G., Pommer, H., Heim, A., 2005. Phylogenetic analysis of the main neutralization and hemagglutination determinants of all human adenovirus prototypes as a basis for molecular classification and taxonomy. *J. Virol.* 79, 15265–15276.
- Madisch, I., Hofmayer, S., Moritz, C., Grntzalis, A., Hainmueller, J., Pring-Akerblom, P., Heim, A., 2007. Phylogenetic analysis and structural predictions of human adenovirus penton proteins as a basis for tissue-specific adenovirus vector design. *J. Virol.* 81, 8270–8281.
- Mahmood, K., Ahmed, W., Farooq, S., Habib, G., Sindhu, M.A., Asif, A., Iftner, T., 2024. Molecular characterization of human adenoviruses associated with pediatric respiratory infections in Karachi, Pakistan. *BMC Infect. Dis.* 24, 538.
- Mao, N., Zhu, Z., Rivallier, P., Chen, M., Fan, Q., Huang, F., Xu, W., 2017. Whole genomic analysis of two potential recombinant strains within Human mastadenovirus species C previously found in Beijing, China. *Sci. Rep.* 7, 15380.
- Mao, N., Zhu, Z., Rivallier, P., Yang, J., Li, Q., Han, G., Yin, J., Yu, D., Sun, L., Jiang, H., Zhan, Z., Xiang, X., Mei, H., Wang, X., Zhang, B., Yu, P., Li, H., Lei, Z., Xu, W., 2019. Multiple divergent Human mastadenovirus C co-circulating in mainland of China. *Infect. Genet. Evol.* 76, 104035.
- Roberts, R.J., O'Neill, K.E., Yen, C.T., 1984. DNA sequences from the adenovirus 2 genome. *J. Biol. Chem.* 259, 13968–13975.
- Rowe, W.P., Huebner, R.J., Gilmore, L.K., Parrott, R.H., Ward, T.G., 1953. Isolation of a cytopathogenic agent from human adenoids undergoing spontaneous degeneration in tissue culture. *Proc Soc Exp Biol Med* 84, 570–573.
- Saha, R., Majumdar, A., Chaudhuri, R.D., Chatterjee, A., Lo, M., Dutta, S., Chawla-Sarkar, M., 2023. Molecular epidemiology of circulating human adenoviruses among acute respiratory infection patients seeking healthcare facilities in West Bengal, India. *Virology* 588, 109912.
- Seto, D., Chodosh, J., Brister, J.R., Jones, M.S., 2011. Using the whole-genome sequence to characterize and name human adenoviruses. *J. Virol.* 85, 5701–5702.
- Takahashi, K., Gonzalez, G., Kobayashi, M., Hanaoka, N., Carr, M.J., Konagaya, M., Nojiri, N., Ogi, M., Fujimoto, T., 2019. Pediatric infections by human mastadenovirus C Types 2, 89, and a Recombinant Type detected in Japan between 2011 and 2018. *Viruses* 11, 1131.
- Walsh, M.P., Chintakuntlawar, A., Robinson, C.M., Madisch, I., Harrach, B., Hudson, N. R., Schnurr, D., Heim, A., Chodosh, J., Seto, D., Jones, M.S., 2009. Evidence of molecular evolution driven by recombination events influencing tropism in a novel human adenovirus that causes epidemic keratoconjunctivitis. *PLoS One* 4, e5635.
- Wang, F., De, R., Han, Z., Xu, Y., Zhu, R., Sun, Y., Chen, D., Zhou, Y., Guo, Q., Qu, D., Cao, L., Liu, L., Zhao, L., 2024. High-frequency recombination of human adenovirus in children with acute respiratory tract infections in Beijing, China. *Viruses* 16, 828.
- Wang, L.Y., Liu, Z.Y., Yin, J.J., Yan, L.W., Wang, P.P., Shi, Y.S., Zhang, Y., Zhao, H.M., 2023. Analysis of the common respiratory viruses in children with acute respiratory infection in a hospital in Lanzhou City from 2021 to 2022. *Chin. J. Prev. Med.* 57, 1635–1639 (in Chinese).
- Wang, Y., Li, Y., Lu, R., Zhao, Y., Xie, Z., Shen, J., Tan, W., 2016. Phylogenetic evidence for intratypic recombinant events in a novel human adenovirus C that causes severe acute respiratory infection in children. *Sci. Rep.* 6, 23014.
- Wei, J., Zang, N., Zhang, J., He, Y., Huang, H., Liu, X., Xu, X., Ren, L., Deng, Y., Wu, J., Seto, D., Zhong, W., Zhang, Q., Liu, E., 2023. Genome and proteomic analysis of risk factors for fatal outcome in children with severe community-acquired pneumonia caused by human adenovirus 7. *J. Med. Virol.* 95, e29182.
- Wu, C., Zhang, Y., Liang, A., Wu, X., Zhu, Y., Huang, Z., Wang, J., Deng, Y., Pan, L., Wang, A., Deng, F., Xia, J., 2025. Comparative analysis between genotypes of adenovirus isolates from hospitalized children with acute respiratory tract infections and clinical manifestations in Wuhan, China, from June 2022 to September 2023. *Virol. Sin.* 40, 50–60.
- Yang, J., Mao, N., Zhang, C., Ren, B., Li, H., Li, N., Chen, J., Zhang, R., Li, H., Zhu, Z., Xu, W., 2019. Human adenovirus species C recombinant virus continuously circulated in China. *Sci. Rep.* 9, 9781.
- Zhao, M.C., Guo, Y.H., Qiu, F.Z., Wang, L., Yang, S., Feng, Z.S., Li, G.X., 2020. Molecular and clinical characterization of human adenovirus associated with acute respiratory tract infection in hospitalized children. *J. Clin. Virol.* 123, 104254.
- Zhu, Z., Mao, N.Y., 2022. Current situation of etiological research on human adenovirus infection. *Infect Dis Info* (35), 206–213+227 (in Chinese).